BIOCHEMISTRY
including biophysical chemistry & molecular biology

Article

pubs.acs.org/biochemistry

Structure and Activity of the *Streptomyces coelicolor* A3(2) β-*N*-Acetylhexosaminidase Provides Further Insight into GH20 Family Catalysis and Inhibition

Nhung Nguyen Thi,[†,‡,§,⊥,∥] Wendy A. Offen,[○] François Shareck,[†] Gideon J. Davies,[○] and Nicolas Doucet*[,†,‡,§]

[†]INRS-Institut Armand-Frappier, Université du Québec, 531 Boul. des Prairies, Laval, Québec H7V 1B7, Canada

[‡]PROTEO, the Québec Network for Research on Protein Function, Structure, and Engineering, 1045 Avenue de la Médecine, Université Laval, Québec, Québec G1V 0A6, Canada

[§]GRASP, the Groupe de Recherche Axé sur la Structure des Protéines, 3649 Promenade Sir William Osler, McGill University, Montréal, Québec H3G 0B1, Canada

[⊥]Military Institute of Science and Technology, 17 Hoang Sam, Hanoi, Vietnam

[∥]Vietnam Academy of Science and Technology, 18 Hoang Quoc Viet, Hanoi, Vietnam

[○]Structural Biology Laboratory, Department of Chemistry, University of York, York YO10 5DD, United Kingdom

Supporting Information

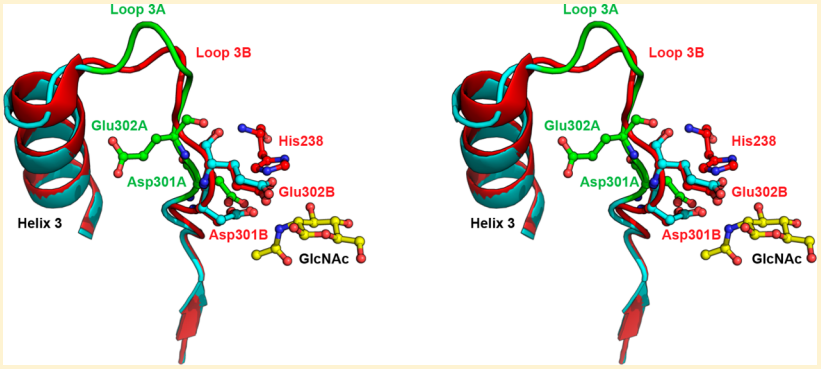

ABSTRACT: β-*N*-acetylhexosaminidases (HEX) are glycosidases that catalyze the glycosidic linkage hydrolysis of *gluco*- and *galacto*-configured *N*-acetyl-β-D-hexosaminides. These enzymes are important in human physiology and are candidates for the biocatalytic production of carbohydrates and glycomimetics. In this study, the three-dimensional structure of the wild-type and catalytically impaired E302Q HEX variant from the soil bacterium *Streptomyces coelicolor* A3(2) (*Sc*HEX) were solved in ligand-free forms and in the presence of 6-acetamido-6-deoxy-castanospermine (6-Ac-Cas). The E302Q variant was also trapped as an intermediate with oxazoline bound to the active center. Crystallographic evidence highlights structural variations in the loop 3 environment, suggesting conformational heterogeneity for important active-site residues of this GH20 family member. The enzyme was investigated for its β-*N*-acetylhexosaminidase activity toward chitooligomers and *p*NP-acetyl *gluco*- and *galacto*-configured *N*-acetyl hexosaminides. Kinetic analyses confirm the β(1−4) glycosidic linkage substrate preference, and HPLC profiles support an exoglycosidase mechanism, where the enzyme cleaves sugars from the nonreducing end of substrates. *Sc*HEX possesses significant activity toward chitooligosaccharides of varying degrees of polymerization, and the final hydrolytic reaction yielded pure GlcNAc without any byproduct, promising high applicability for the enzymatic production of this highly valued chemical. Thermostability and activation assays further suggest efficient conditions applicable to the enzymatic production of GlcNAc from chitooligomers.

β-*N*-acetylhexosaminidases (HEX, E.C. 3.2.1.52) are glycosidases that hydrolyze the glycosidic linkage of both *gluco*- and *galacto*-configurations of *N*-acetyl-β-D-hexosaminides, which are found in oligosaccharides, glycoproteins, glycolipids, and glycosaminoglycans. HEX members have been extensively studied due to their physiological and functional roles in bacteria, fungi, insects, plants, and mammals.[1] These enzymes have also attracted considerable attention due to their importance in human diseases; defects in human lysosomal HEX causes neurodegenerative Tay-Sachs and Sandhoff

Received: December 23, 2013
Revised: February 19, 2014
Published: February 21, 2014

   dx.doi.org/10.1021/bi401697j | *Biochemistry* 2014, 53, 1789−1800

Scheme 1. Proposed Catalytic Mechanism of *Sc*HEX (Based on Ref 1, See Text for Details)

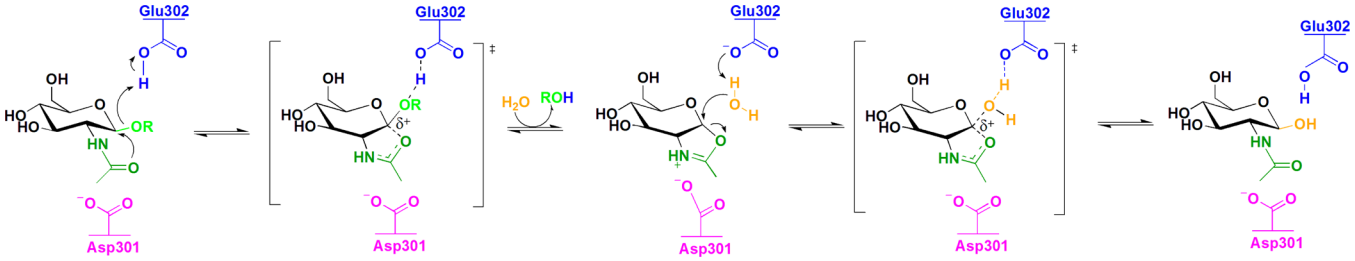

diseases.[2] Additionally, they have been used as a means to control fungal and insect pests, in addition to being efficient tools for a number of biotechnological applications.[1] Based on amino acid sequence similarity, the Carbohydrate-Active Enzyme Database (CAZy, http://cazy.org/) classifies HEX members into four distinct families: GH3, GH20, GH84, and GH85. The GH20 family has been thoroughly characterized with respect to substrate specificity, structure, catalytic mechanism, and biosynthetic potential.[1] GH20 members have the ability to cleave a broad range of substrates, including $\beta(1-4)$, $\beta(1-3)$, $\beta(1-2)$, and/or $\beta(1-6)$ glycosidic linkages, as well as branched compounds such as glycoproteins, glycolipids, or sulfated glycoconjugates.[3−8] To date, a number of GH20 crystal structures have been resolved, including bacterial, insect, and human enzymes.[1,9] The catalytic domain of all members presents a highly similar $(\beta/\alpha)_8$-barrel (TIM-barrel) architecture, with structural differences lying mainly in subunit organization.[1]

The catalytic mechanism of GH20 enzymes has also been extensively investigated. The enzymes use a double-displacement retaining mechanism with neighboring group participation (Scheme 1).[1] In the first part of the reaction, the carbonyl oxygen of the terminal 2-acetamido substrate moiety acts as a nucleophile, yielding a bicyclic oxazoline (or oxazolinium ion as shown in Scheme 1) intermediate, aided by a conserved aspartate residue (D301 in *Sc*HEX), and with protonic assistance to leaving group departure provided by a conserved acid/base (E302 in *Sc*HEX). In the second step, the catalytic base activates the incoming nucleophile (water, or another sugar in the case of transglycosylation reactions) to form the reaction product.[1,10,11]

GH20 enzymes have been used for the synthesis of carbohydrates and glycomimetics in a number of biotechnological applications. In particular, they can hydrolyze chitooligomers generated from the chitin degradation process to produce *N*-acetyl-D-glucosamine (GlcNAc), a monosaccharide with significant added value in the medical and cosmetic fields.[12] In recent years, enzymatic processes have gained efficiency at replacing harsh and environmentally damaging chemical processes for the industrial production of GlcNAc.[13] However, several issues remain with this production method, which are mainly caused by product purity and productivity.[14,15] There is therefore impetus for investigating diverse HEX enzymes that may result in more efficient production of GlcNAc.

The *Streptomyces* species are well-known chitinolytic organisms. *Streptomyces coelicolor* A3(2) is a Gram-positive bacterium that produces many different hydrolases, including chitinases and *N*-acetylhexosaminidases.[16,17] The sequenced genome of *S. coelicolor* A3(2) reveals 13 putative chitinases and 11 putative HEX members.[18] It is known that HEX and chitinases act in a concerted fashion to degrade chitin fully.[19,20] Previous genetic studies have revealed that, in the presence of colloidal chitin and/or $(GlcNAc)_2$, *S. coelicolor* A3(2) secretes chitinases to degrade chitin into chitooligomers, which are subsequently hydrolyzed by HEX to produce GlcNAc in vivo.[21,22] To date, numerous studies have focused on the importance of *S. coelicolor* A3(2) chitinases,[16,17,23−25] but less attention has been paid to the *N*-acetylhexosaminidase activity. The goal of the present study was to clarify the chitinolytic system of *S. coelicolor* A3(2) by providing detailed structural, kinetics, and stability characterization of the *β*-*N*-acetylhexosaminidase activity from *S. coelicolor* A(3)2. Here, we report the cloning and expression of the *S. coelicolor* A3(2) SCC105.17c *hex* gene and the kinetic and structural characterization of the resulting protein. *Sc*HEX possesses significant activity toward chitooligosaccharides of varying degrees of polymerization, and the final hydrolytic reaction yielded pure GlcNAc without any byproduct, promising high applicability for the enzymatic production of GlcNAc. Additional factors such as enzyme preincubation with small saccharides also proved efficient in activating enzyme efficiency.

EXPERIMENTAL PROCEDURES

Reagents. All reagents used were of the highest commercial purity available. Restriction enzymes and DNA-modifying enzymes were purchased from New England Biolabs and Roche Diagnostics. Chitooligosaccharides $[(GlcNAc)_n; n = 1-6]$ were purchased from V-Laboratories. *p*NP-*N*-acetylgalactosamine was purchased from Gold Biotechnology. 4-Nitrophenyl *N*-*N*′-diacetylchitobioside $[(GlcNAc)_2$-*p*NP], 4-nitrophenyl *N*-acetyl glucosaminide [(GlcNAc)-*p*NP], *p*NP-pyranosides, and practical-grade crab shell chitin were purchased from Sigma-Aldrich. Cell wall peptidoglycan from the Gram-positive *Bacillus subtilis* and *Streptomyces sp.* were also purchased from Sigma-Aldrich. Glycol chitin-80 (80% acetylated) was prepared as previously described.[26] Chitosan-24 (24% acetylated) was obtained from HaloSource. 6-Acetamido-6-deoxy-castanospermine (6-Ac-Cas) was purchased from GlycoSyn, Industrial Research Limited, New Zealand and di-*N*-acetyl-chitobiose $(GlcNAc)_2$ from Seikagaku Biobusiness, Japan. The strain *S. lividans* IAF 10-164 [*msiK*$^-$] was used for all protein expressions.[27]

Cloning of *Sc*HEX. All molecular biology procedures and DNA manipulations in *S. lividans* were performed according to standard published methods.[28] The gene encoding for the *β*-*N*-acetylhexosaminidase from *Streptomyces coelicolor* A3(2) (SCC105.17c) was amplified by PCR using the following DNA primers: 5′-AAAGCATGCGACCTCATCGACGGCACCACAGAA-3′ (forward), coding for the ATG start codon within a *Sph*I restriction site (underlined), and 5′-TTTGAGCTCTCAGGTCCAGGGCACCTG-3′ (reverse),

dx.doi.org/10.1021/bi401697j | *Biochemistry* 2014, 53, 1789−1800

Table 1. Data Collection, Refinement, and Structure Quality Statistics for *Sc*HEX and Complexes

	*Sc*HEX	*Sc*HEX-6-Ac-Cas	E314Q-*Sc*HEX-NGO
resolution of data (outer shell), Å	52.24−1.85 (1.95−1.85)	48.95−2.0 (2.10−2.0)	41.35−1.80 (1.90−1.80)
space group	$P2_12_12_1$	$P2_12_12_1$	$P2_12_12_1$
unit cell params	a = 72.7 Å	a = 72.8 Å	a = 58.2 Å
	b = 128.9 Å	b = 129.2 Å	b = 64.5 Å
	c = 150.3 Å	c = 149.9 Å	c = 143.7 Å
	$\alpha = \beta = \gamma = 90°$	$\alpha = \beta = \gamma = 90°$	$\alpha = \beta = \gamma = 90°$
R merge[a] (outer shell)	0.064 (0.56)	0.17 (0.53)	0.10 (0.51)
mean I/sI (outer shell)	16.8 (3.3)	8.8 (3.2)	12.2 (3.5)
completeness (outer shell), %	99.9 (99.9)	99.4 (98.6)	100.0 (100.0)
multiplicity (outer shell)	6.1 (6.2)	5.6 (5.7)	7.1 (7.3)
no. unique reflns	120 786	95 616	50 954
R_{cryst}	0.17	0.16	0.18
R_{free}	0.20	0.18	0.21
no. protein atoms	7870	7847	3903
no. ligand atoms	0	32 (6-Ac-Cas)	14 (NGO)
no. solvent waters	904	1150	456
no. EDO[b] atoms	88	136	44
Rmsd for bonds (Å)	0.019	0.019	0.019
Rmsd for angles (°)	1.883	1.854	1.814
rmsd chiral volume (Å^3)	0.149	0.137	0.145
average protein B factor (Å^2)	27	11	19
average main chain B factor (Å^2)	26	10	18
average side chain B factor (Å^2)	28	11	20
average B factor for ligand/EDO (ligand only) (Å^2)	43	22 (9)	28 (18)
average solvent B factor (Å^2)	39	24	29
PDB entry	4C7D	4C7F	4C7G

[a] $R_{merge} = \Sigma_{hkl}\Sigma_i\backslash Ihkli - \langle I_{hkl}\rangle / \Sigma_{hkl}\Sigma_i\backslash I_{hkli}$. [b] EDO is ethylene glycol.

coding for a TGA stop codon and a *Sac*I restriction site (underlined). The *Sac*I−*Sph*I-digested PCR product was ligated into the 5.3 kb *Sac*I−*Sph*I-digested pC109 plasmid, which carries a thiostrepton resistance marker. The resulting construct was used to transform *Streptomyces lividans* 10-164 protoplasts and plated on R5 medium without antibiotic for 16 h at 34 °C, at which point agar plates were flooded with thiostrepton solution and further incubated 3−4 days at 34 °C. The 6.9 kbp plasmid was isolated, and positive clones were confirmed by DNA sequencing. The E302Q mutation was introduced by overlap extension PCR[29] using the following DNA primers: 5′-AAAGCATGCCGCTACCTGCACATCGGCGGCGAC-CAGGCGCACTCCACGCCGCAGGCC-3′ (forward) and 5′-TTTGAGCTCGGCCTGCGGCGTGGAGTGCG-GACCGTCGCCGCCGATGTGCAGGTAGCGGC-3′ (reverse).

Gene Expression and Protein Purification. Expression of the *Sc*Hex gene was performed in *S. lividans* 10-164 using slight modifications of previously published methods.[28] Strains were cultivated in 500 mL Erlenmeyer flasks for 72 h at 34 °C with agitation (250 rpm) in M14 medium supplemented with 1% xylose (w/v) as the sole carbon source. Mycelium was removed by centrifugation, and the supernatant was filtered through a 0.2 μm Whatman nylon membrane (GE Healthcare). The protein solution was concentrated by ultrafiltration and dialyzed against 10 mM citric buffer, pH 4.5 prior to loading onto a Protein-Pak HR CM-8 AP-1 column (Waters) pre-equilibrated with 10 mM citric buffer, pH 4.5. *Sc*HEX was eluted with a linear gradient of 10 mM citric buffer, pH 4.5 containing 1 M NaCl, and protein elution was monitored at 280 nm. Fractions containing *Sc*HEX were pooled after analysis by SDS-PAGE, and mass spectrometry was used to assess purity. Total protein concentration was determined using a Bio-Rad Protein Assay (Bio-Rad).

Mass Spectrometry. SDS-PAGE protein bands were excised and destained with water/sodium bicarbonate buffer and acetonitrile. Before in-gel digestion with trypsin, proteins were reduced by DTT and alkylated with iodoacetamide. The tryptic peptides were eluted and then separated on an Agilent Nanopump using a trap column (ZORBAX 300 SB-C18) and a reverse-phase column (ZORBAX 300 SB-C18, 150 mm × 75 μm, 3.5 μm particle size) (Agilent). Mass spectra were obtained using a Q-trap mass spectrometer (Applied Biosystems/MDS SCIEX instruments) equipped with a nanoelectrospray ionization source. Accumulation of MS-MS data was performed with the Analyst Software, version 1.4 (Applied Biosystems/MDS SCIEX). MASCOT (Matrix Science) was used for database searching.

Crystallization, Data Collection, and Structure Solution. Freeze-dried protein was solubilized in 10 mM CHES buffer, pH 9.5, and crystallized using the hanging drop method, with the drop containing *Sc*HEX at 5 mg/mL in a ratio of 2.5: 1 with well solution (0.1 M HEPES pH 7.3, 8% (w/v) PEG 6000). The crystal was fished via a cryoprotectant, which comprised the well solution supplemented with 25% (v/v) ethylene glycol, into liquid nitrogen. Data were collected at beamline IO3, Diamond, to 1.85 Å, at 100 K. Structure solution used the CCP4 suite of programs.[30] The structure was solved by Molecular Replacement with PHASER,[31] using PDB entry 1HP4 as a model (94% sequence identity).[10] The model was improved by iterative cycles of manual building in COOT,[32] followed by refinement with REFMAC.[33]

For the complex with 6-acetamido-6-deoxy-castanospermine (6-Ac-Cas), a crystal which had grown after 4 weeks in a

dx.doi.org/10.1021/bi401697j | *Biochemistry* 2014, 53, 1789−1800

hanging drop, comprising protein at approximately 7 mg/mL in 50 mM HEPES pH 7.5, 0.2 M NaCl, 20 mM CHES pH 9.3, mixed 1:1 with well solution consisting of 0.1 M BIS-TRIS pH 6.5, 4% (w/v) PEG 6000, 5% DMSO, was soaked with a speck of solid 6-Ac-Cas introduced around the crystal with a needle. Following soaking for approximately 40 min, the crystal was fished via cryoprotectant (as above). Data were collected at beamline IO2, Diamond, to 2 Å resolution, although the crystal was of poor quality reflected by a relatively high R_{merge}. The structure was refined using the (isomorphous) wild-type structure as the starting model, using REFMAC and COOT.

A crystal of the site-directed mutant E302Q, initially in complex with the disaccharide di-*N*-acetyl-chitobiose $(GlcNAc)_2$, was crystallized at 5 mg/mL in 10 mM CHES pH 9.5, mixed 1:0.8 with well solution comprising 0.1 M HEPES pH 7.0, 4% (w/v) PEG 6000. A small amount of solid $(GlcNAc)_2$ powder was added to the protein drop, and the crystal was fished after 5 days via 6% (w/v) PEG 6000, 0.1 M HEPES pH 7.0, 25% (v/v) ethylene glycol also supplemented with 20 mM $(GlcNAc)_2$. Data were collected at beamline IO4 Diamond, to 1.8 Å resolution. The structure was solved using PHASER, with the wild-type structure as the search model and refined as above. Upon structure solution it became immediately apparent that the ligand bound was the trapped intermediate GlcNAc (NAG)−oxazoline (NGO) rather than the intact substrate (see below). Data collection and structure refinement statistics are given in Table 1.

β-*N*-Acetylhexosaminidase Activity. β-*N*-acetylhexosaminidase activity against *p*-nitrophenyl β-*N*-acetylhexosaminides and *p*-nitrophenyl pyranosides was determined by continuous spectrophotometric assays by measuring the release of *p*-nitrophenol at 405 nm on a Cary 300 Bio spectrophotometer (Agilent) equipped with a circulating heating water bath (Lauda). Reactions were carried out at 55 °C for 10 min in 50 mM phosphate buffer containing 150 mM NaCl (pH 5.5). Activity was expressed in IU/mg of protein (1 IU = 1 μmole of *p*-nitrophenol released per minute). Determination of *Sc*HEX enzyme activity toward chitooligosaccharides was performed by an isocratic HPLC method in the same buffer conditions. Aliquots (100 μL) were taken at various time intervals and mixed with 100 μL of 0.4 M H_2SO_4 to quench the reaction. Samples (100 μL) were subsequently injected on an Aminex HPX-87H Ion Exclusion Column (7.8 mm × 30 cm) (Bio-Rad), and elution was performed in isocratic mode with a mobile phase of 5 mM H_2SO_4 at a flow rate of 0.5 mL/min (45 °C). Identification of molecular species was performed by comparison with the retention time of known standards, and product concentrations were calculated from HPLC peak areas. Activity was expressed in IU/mg of protein (1 IU = 1 μmole of GlcNAc released per minute). The growth supernatant of a pC109-transformed *S. lividans* 10-164 subjected to the same gene expression protocol was used as a mock control for all enzyme assays.

Substrate Specificity. Substrate specificity of the purified *Sc*HEX was determined using chromogenic compounds *p*NP-GlcNAc, *p*NP-GalNAc, and *p*NP-pyranosides, in addition to natural chitins and chitooligosaccharides of varying degrees of polymerization $[(GlcNAc)_n;\ n = 1-6]$. To investigate the activity toward long chain chitins, enzyme assays were carried out in the aforementioned buffer using either 2.5 mg/mL of 80% glycol chitin, 40% glycol chitin, 24% chitosan, chitin crabshell, colloidal chitin or 1 mg/mL peptidoglycan from *Streptomyces sp*. or *Bacillus subtilis*. To initiate the reaction, the purified enzyme was added to a final concentration of 10 μg/mL. Reactions were performed for 24 h with aliquots taken after 18h and 24h of incubation at 55 °C. Products were detected at 210 nm by an isocratic HPLC ion exclusion method using an Aminex HPX-42A column (7.8 mm × 30 cm) (Bio-Rad). Elution was performed with H_2O as the mobile phase at a flow rate of 0.5 mL/min (45 °C). In all cases, control assays were also performed with water and a mock supernatant.

Optimal pH, Temperature, and Stability. Optimal temperature for *Sc*HEX was determined in 50 mM phosphate buffer containing 150 mM NaCl with chitooligosaccharides $[(GlcNAc)_n;\ n = 1-6]$ as substrates. Enzyme assays were performed for 10 min at 25, 30, 37, 40, 45, 50, 55, 60, 65, and 70 °C. The optimal pH for chitooligosaccharide hydrolysis was determined at 55 °C by performing the same enzyme assays in 50 mM citric buffer with 150 mM NaCl (pH 3, 3.5, 4, 4.5), 50 mM phosphate buffer with 150 mM NaCl (pH 5, 5.5, 6, 6.5, 7), and 50 mM Tris-HCl buffer with 150 mM NaCl (pH 8). Reactions were carried out for 10 min, and enzyme activity was calculated as mentioned above. The pH stability and thermal stability of *Sc*HEX were estimated by incubating enzyme solutions (100 μL, 200 μg/mL) at different pHs (1h and 3 months at 4 °C) and temperatures (15 min) prior to initiating enzyme reaction with *p*NP-GlcNAc, as described above. Activity was compared to a control, which was performed with pure enzyme kept in water at 4 °C.

Michaelis−Menten Kinetics. The kinetic parameters k_{cat} and K_M were determined at 55 °C and optimal pH in 50 mM phosphate buffer, 150 mM NaCl for chitooligosaccharide substrates $[(GlcNAc)_n;\ n = 1-6]$. Enzyme assays were initiated by the addition of 0.5 μg/mL *Sc*HEX with substrate concentrations ranging from 0.25 to 3 mM. *Sc*HEX activity was calculated as μmoles of GlcNAc released per minute per milligram of enzyme, and kinetic parameters k_{cat}, K_M and k_{cat}/K_M were calculated by a nonlinear regression fit to the Michaelis−Menten equation using GraphPad Prism 5.

Carbohydrate Activation/Inhibition. The effect of potential activators and inhibitors on β-*N*-acetylhexosaminidase activity was examined by preincubating enzyme solutions (100 μL, 200 μg/mL) with 3 mM of the following carbohydrates for 15 min prior to reaction initiation: mannose, fructose, arabinose, glucuronic acid, sucrose, galactose, glucose, xylose, lactose, and GlcNAc. Enzyme assays were carried out with *p*NP-GlcNAc as described above, and sugars were prepared in the same reaction buffer. Activities were compared to a control of pure *Sc*HEX performed under the same reaction conditions but preincubated in the absence of any sugar.

RESULTS AND DISCUSSION

***Sc*HEX Expression, Purification, and Structural Analysis.** *Sc*HEX was produced from a culture of *S. lividans* grown in M14 minimal medium containing xylose as the sole source of carbon. Under these conditions, *Sc*HEX was overproduced with an expression yield of 700−800 mg/L after 72 h incubation. The *S. lividans* expression system allows extracellular secretion of *Sc*HEX with an extremely low background of contaminant proteins, yielding an enzyme purity of 95% directly from the growth supernatant. Ion-exchange chromatography was nevertheless employed to purify enzymes to homogeneity, and mass spectrometry was employed to confirm the identity and sequence integrity of the produced enzyme. To rule out the possibility of a contaminant GH activity, the strain *S. lividans* 10-164 with empty plasmid pC109 was cultured to test the

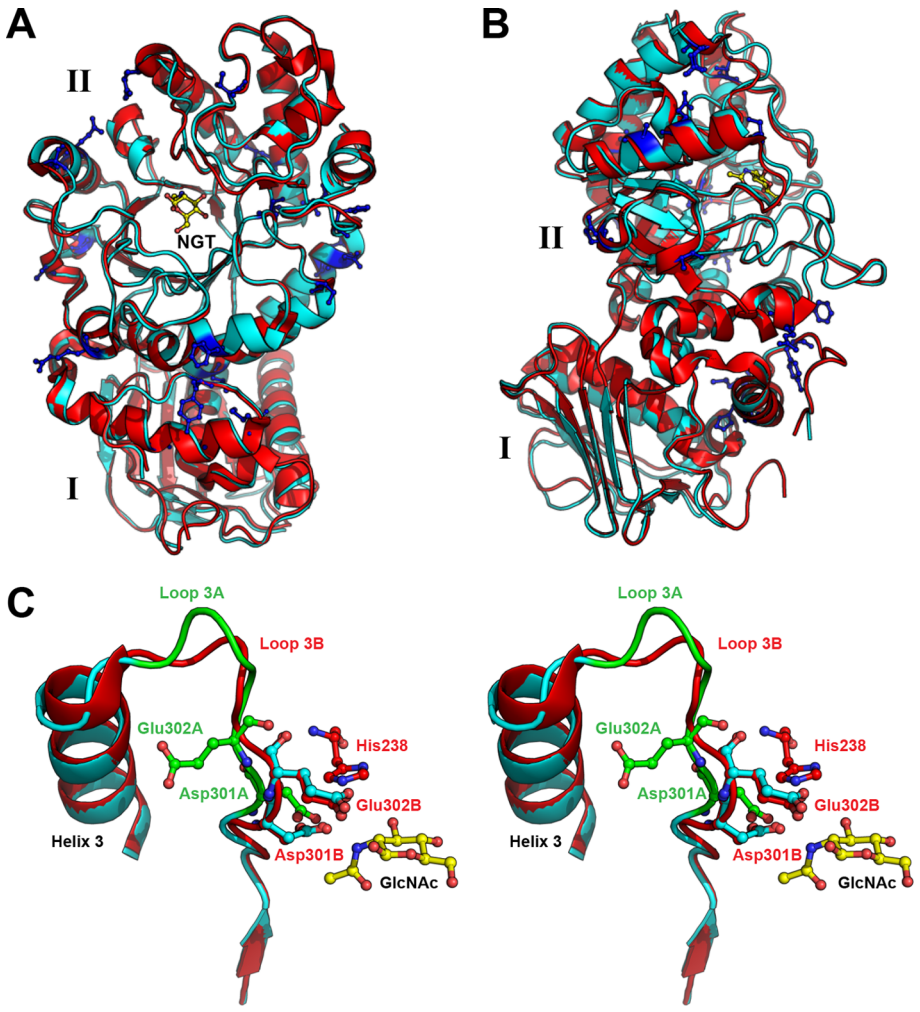

Figure 1. Structural comparison between *Sp*HEX and *Sc*HEX. (A) Front-view overlay of wild-type *Sp*HEX (PDB entry 1HP5, red) with wild-type *Sc*HEX (PDB entry 4C7D, cyan). The position of the active site is defined by the presence of NAG−thiazoline bound within the *Sp*HEX binding pocket (NGT, yellow). The β/α topology domain I and $(\beta/\alpha)_8$ barrel domain II are identified by roman numerals. Residues of the $(\beta/\alpha)_8$ barrel comprising catalytic domain II that differ in sequence between *Sp*HEX and *Sc*HEX are shown in ball-and-stick representation in *Sc*HEX (blue). (B) Side-view of the complex (90° counter clockwise rotation about the *y*-axis relative to (A)). (C) Stereo view of *Sp*HEX (PDB entry 1M01, red) and *Sc*HEX (cyan/green) showing two alternate conformations adopted by loop 3 in *Sc*HEX. Positions of the modeled loop 3 conformations A (0.7 occupancy) and B (0.3 occupancy) are shown in green and red, respectively. The loop 3B conformation corresponds to the active orientation of catalytic residues Asp301B and Glu302B (cyan in *Sc*HEX and red in *Sp*HEX), which are ideally positioned to hydrogen bond with glycans in the active-site pocket. Residues Asp301A and Glu302A in conformation A are shown in green. The *N*-acetylglucosamine (GlcNAc) product complexed to *Sp*HEX is shown in yellow. This figure was drawn with MacPyMOL 1.3.

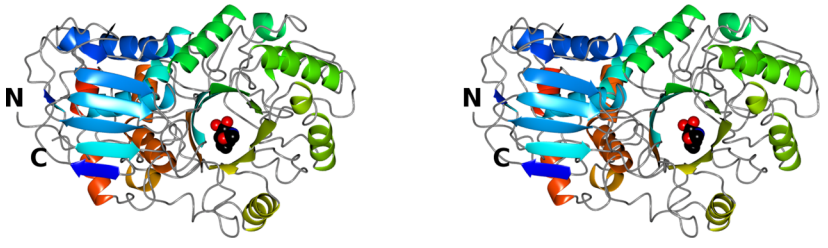

Figure 2. Stereo view of a ribbon diagram of *Sc*HEX. The enzyme is color-ramped from the N-terminus (blue) to C-terminus (red), showing the position of 6-Ac-Cas as a CPK model. This figure was drawn with CCP4*mg*.[52]

growth supernatant for acetylhexosaminidase activity against $(GlcNAc)_2$ and $(GlcNAc)_6$. Results showed no activity toward these substrates, ruling out the possibility of a contaminant HEX activity in the cell extract of the expression host.

Amino acid sequence alignment of *Sc*HEX with other GH20 family members exhibits 99%, 94%, 77%, 60%, 43%, and 27% sequence identity with *S. lividans*, *S. plicatus*, *S. avermitilis*, *Saccharopolyspora erythraea*, *Paenibacillus sp.*, and *Homo sapiens* (HEXB), respectively (Figure S1). Like other members of the family, *Sc*HEX retains the highly conserved active site motif His/Asn-X_{aa}-Gly-Ala/Cys/Gly/Met-Asp-Glu-Ala/Ile/Leu/Val, in which a glutamate residue (E302 in *Sc*HEX) acts as the

dx.doi.org/10.1021/bi401697j | *Biochemistry* 2014, 53, 1789−1800

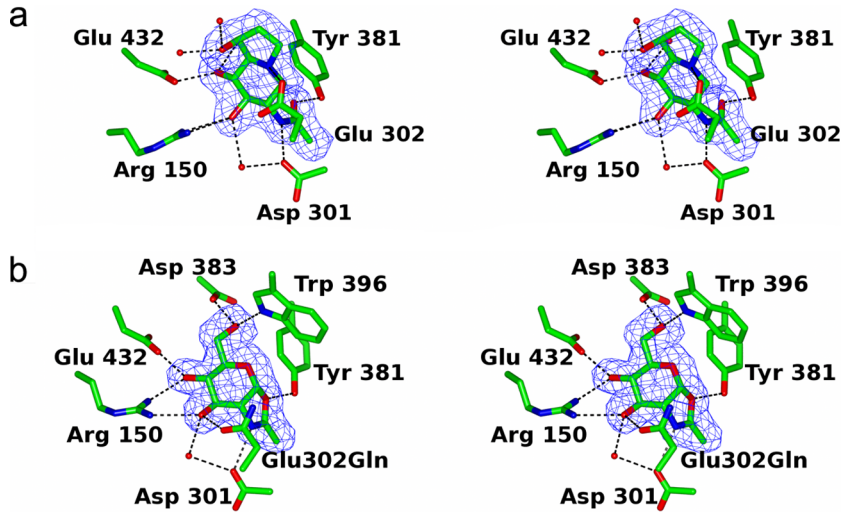

Figure 3. Stereo views (divergent "wall-eyed" stereo) of the *Sc*HEX 6-Ac-Cas and E302Q *Sc*HEX NAG−oxazoline active-site complexes. F_o-F_c omit electron density maps (with phases calculated *prior* to any modeling or refinement of any ligand) of each complex are shown in blue, contoured at 3.0 σ. (A) *Sc*HEX 6-Ac-Cas complex (molecule A). (B) E302Q *Sc*HEX NAG−oxazoline complex. Hydrogen bonds ≤3.2 Å are shown as dashed lines. This figure was drawn with CCP4*mg*.

general acid/base in the catalytic mechanism.[34] The closest HEX homologue for which a crystal structure was previously solved is the GH20 β-*N*-acetylhexosaminidase from *S. plicatus* (*Sp*HEX), an enzyme displaying 94% sequence identity with *Sc*HEX.[10] As expected, this high similarity between the two enzymes results in very similar three-dimensional structures, discussed below. This is in agreement with the fact that the catalytic domains of *Sp*HEX and *Sc*HEX only differ at 21 out of 355 residue positions. None of these replacements occur at positions in or near the active site cavity and/or involved in catalysis (Figure S1, Figure 1A,B), confirming that both enzymes rely on the same catalytic mechanism and display similar substrate specificities.

Structure of *Sc*HEX, and Complexes *Sc*HEX-6-Acetamido-6-deoxy-castanospermine and E302Q *Sc*HEX-NAG−oxazoline. The structure of *Sc*GH20 has a very similar two domain architecture to that of *Sp*HEX, with an N-terminal domain (up to Arg138) consisting predominantly of a solvent-exposed seven-stranded β-sheet, sequestering two α-helices against the C-terminal domain, which comprises a $(\beta/\alpha)_8$ barrel with an additional α-helix near the C terminus occupying the groove between the two domains (Figure 2).[10] The barrel motif is irregular, in that helix 7 is replaced by a loop, helix 5 is very short, and there are 2 additional loops at the C-termini of β-strands 2 and 3. There are two molecules in the asymmetric unit for the native structure, and the complex with 6-Ac-Cas, designated A and B in the PDB entries, and one for that of the mutant E302Q soaked with $(GlcNAc)_2$, which has NAG−oxazoline in the active site.

In molecule A of the native structure, residues 299−308 on loop 3 follow a different pathway to the equivalent residues in both complex structures (Figure 1C). In molecule B, the same region has two alternate conformations, A and B, with partial occupancies of 0.7 and 0.3, respectively. Conformation A is the same as that observed for molecule A, and loop conformation B is equivalent to that observed in both ligand-bound structures and the structure of *Sp*HEX bound to GlcNAc (PDB entry 1M01).[11] The main difference is in the orientations of the side chains of Asp301, Glu302 (both catalytic residues) and Ala303. In conformation B, and both complexes, the side chains of residue 302 are hydrogen bonded to NE2 of His238, but in the native structure, molecule A and conformation A of region 299−308 on molecule B, the side chain of Glu302 points away from, and cannot hydrogen bond to the histidine. This alternate ligand-bound conformation facilitates the formation of hydrogen bonding interactions. In the 6-Ac-Cas structure, OD2 of Asp301 is hydrogen bonded to the nitrogen of the ligand acetamido group (2.8 Å), and OE2 of Glu302 is 2.8 Å from the castanospermine nitrogen atom (Figure 3A). In the complex with NAG−oxazoline, the loop is positioned in such a way that there are hydrogen bonds between OD2 of Asp301 and the nitrogen atom of NAG−oxazoline (2.9 Å), and between OE1 of Gln302 and O3 of NAG−oxazoline (2.8 Å) (Figure 3B). For molecule B of the native structure, the alternate loop conformations differ in some main chain hydrogen bonding interactions, for example the carbonyl O of Asp301B loop in conformation A is hydrogen bonded to the main chain N of Gly237B, whereas in loop B it is hydrogen bonded to that of Ala303B (not shown).

In an attempt to trap a Michaelis complex, the crystal structure of the acid/base variant E302Q was determined in complex with di-*N*-acetyl-chitobiose. In contrast to what was expected, the structure clearly revealed electron density for a trapped intermediate oxazoline in the −1 subsite. In trapping of oxazolines on related GH84 enzymes, He and colleagues[35] used active center variants in conjunction with highly activated substrates; here serendipitously the intermediate has accumulated without the requirement for an activated substrate. As expected, the NAG−oxazoline and active site residues occupy very similar positions to those in the complex of the inhibitor *N*-acetylglucosamine−thiazoline (NAG−thiazoline) with *Sp*HEX (PDB entry 1HP5).

The trapped oxazoline complex, along with the complex with 6-Ac-Cas informs a complete description of the interaction in the −1 subsite. Both ligand sugars are close to a $^4C_1$ conformation. The acetamido group is anchored by hydrogen bonding interactions between its nitrogen atom and OD2 of Asp301, and oxygen and OH of Tyr381 (Figure 3, Scheme 2). The structure of GlcNAc bound to *Sp*HEX exhibits a similar pattern of bonding between the equivalent N and O atoms of

dx.doi.org/10.1021/bi401697j | *Biochemistry* 2014, 53, 1789−1800

Scheme 2. Schematic Diagram of the Interactions between *Sc*HEX and the Intermediate Oxazoline Trapped on the E302Q Variant[a]

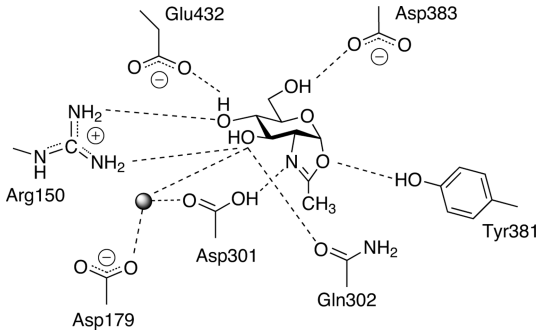

[a]Hydrogen bonding distances ≤3.2 Å are indicated by dashed lines. The water molecule is shown as a shaded sphere.

the ligand and residues Asp313 and Tyr393.[11] Four tryptophan residues, 332, 349, 396 and 430, provide a hydrophobic environment that protects the oxazolinium ion intermediate from solvolysis (Figure 4). The positive charge on the nitrogen of the acetamido group in the NAG−oxazoline complex is likely stabilized by Asp301, which is itself within hydrogen bonding distance of Asp234, and therefore probably deprotonated. The oxygen atom O3 of NAG−oxazoline is 2.8 Å from OE1 of the mutated residue Gln302, and in the 6-Ac-Cas complex N1 of the castanospermine group is hydrogen bonded to OE2 of Glu302 (2.8 Å). Further residues interact, via hydrogen bonding interactions with their side chains, to hold the sugar moiety of both ligands in place as follows: Asp179 (OD2 via a water molecule to O4 of 6-Ac-Cas and O3 of NAG−oxazoline), Arg150 (both terminal guanidinium N atoms with O4 of 6-Ac-Cas, and one each to O3 and O4 NAG−oxazoline), Glu432 (OE2 to O2 of 6-Ac-Cas and O4 of NAG−oxazoline) and Asp383 and Trp396 (OD2 and NE1 respectively *via* a water molecule to O2 of 6-Ac-Cas, directly to O6 of NAG−oxazoline) (Figure 3, Scheme 2). In addition, a water molecule, which is hydrogen bonded to both OD2 Asp301 and OD2 Asp179, forms a hydrogen bond to O4 6-Ac-Cas and to O3 NAG−oxazoline in their respective complexes (3.0 Å in each case).

In the *Sp*HEX NAG−thiazoline complex, a glycerol molecule occupies subsite +1 and forms a hydrogen bond with OE2 Glu314 (2.7 Å). There is an equivalent ethylene glycol molecule in the E302Q *Sc*HEX NAG−oxazoline structure, which lies 2.7 Å from the side chain of Gln302. The wild-type structure also has an ethylene glycol molecule (at half occupancy) in a different orientation, but with a hydroxyl group in a position equivalent to the hydroxyl binding to Gln302 in the NAG−oxazoline structure, and a second ethylene glycol with hydroxyl groups occupying similar positions to NAG−oxazoline O6 and O4.

Enzyme Specificity. Glycoside hydrolases are classified into 130 families based on their amino acid sequence similarities.[36−38] Although members of the GH20 family share a common catalytic domain with conserved active site residues—confirmed by the detailed description of the structure above—they nevertheless show a wide variety of substrate specificities. Overall, GH20 enzymes have the ability to cleave $\beta(1-2)$, $\beta(1-3)$, $\beta(1-4)$, $\beta(1-6)$ glycosidic linkages from oligosaccharides, glycoproteins, glycolipids, and glycosaminoglycans.[8,39−41] The GH20 family also relies on a substrate-assisted mechanism wherein the 2-acetamido group of the substrate is indispensable for catalysis (Scheme 1).[1,10,11,42] To determine the substrate specificity of *Sc*HEX and to confirm its anchimeric mode of action, we tested chromogenic and natural substrates with 2-acetamido groups such as *p*NP-GlcNAc, *p*NP-GalNAc, chitooligosaccharides, and long chain chitins. As expected, the enzyme showed significant activity toward *p*NP-GlcNAc, *p*NP-GalNAc, and chitooligosaccharides (Table 2). The highest specific activity (666 ± 11 IU/mg) was observed with *p*NP-GlcNAc as substrate, which is 2.9-fold higher than that observed with the homologous *p*NP-GalNAc (230 ± 4 IU/mg). This result confirms the D-*gluco* configuration substrate preference of *Sc*HEX, in agreement with the 1.5 to 4 GlcNAcase/GalNAcase activity ratio found in other

Table 2. Specific Activity of *Sc*HEX toward Various *N*-Acetylhexosaminide Substrates

substrate	specific activity (IU)[a]
*p*NP-GlcNAc	666 ± 11[b]
*p*NP-GalNAc	230 ± 4[b]
$(GlcNAc)_6$	180 ± 25
$(GlcNAc)_5$	146 ± 11
$(GlcNAc)_4$	71 ± 6
$(GlcNAc)_3$	122 ± 12
$(GlcNAc)_2$	126 ± 5

[a]IU = μmol/min of GlcNAc released per milligram of enzyme. [b]IU = μmol/min of *p*NP released per milligram of enzyme. Results are presented as means ± standard deviation (n = 3).

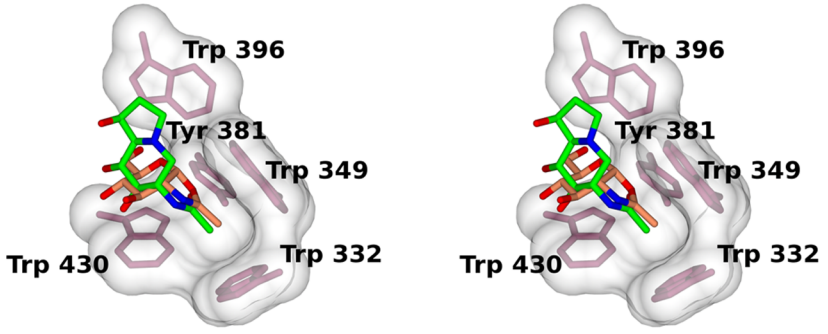

Figure 4. Stereo view of hydrophobic residues in the −1 sugar binding subsite for molecule A of *Sc*HEX complexed with 6-Ac-Cas. The position of NGO is shown when the structure of its complex is superposed on that with 6-Ac-Cas. 6-Ac-Cas is shown with C atoms in green, and NGO is shown in coral. The molecular surface around the hydrophobic residues is shown (calculated by CCP4*mg*).

dx.doi.org/10.1021/bi401697j | *Biochemistry* 2014, 53, 1789−1800

GH20 enzymes.[19] *Sc*HEX also displayed specific activities ranging from 71 to 180 IU/mg toward chitooligosaccharide substrates (Table 2), confirming that the enzyme most likely acts on smaller chain products of chitin degradation *in vivo*. To further investigate the glycosidase activity, time-course profiles for the hydrolysis of $(GlcNAc)_6$ were determined under conditions described above. Time-course analysis of the *Sc*HEX activity toward $(GlcNAc)_6$ yielded a hydrolysis profile whereby $(GlcNAc)_5$ and GlcNAc are released as primary products at the early stage of the reaction, followed by decreasing concentrations of $(GlcNAc)_4$, $(GlcNAc)_3$, and $(GlcNAc)_2$ (Figure 5). The corresponding increase in GlcNAc, the low accumulation of smaller oligomers such as $(GlcNAc)_2$ at the early onset, and the very similar affinity of *Sc*HEX for all chitooligosaccharides (see below) confirms that the enzyme acts in a processive manner, trimming off GlcNAc units from the nonreducing ends of substrates of varying degrees of polymerization, as previously demonstrated on homologues.[3,5,43] The same cleavage pattern was observed when $(GlcNAc)_{2-5}$ chitooligomers were used as substrates, with the appearance of $n-1$ products at an early stage of the reaction, concomitant with gradual increases in GlcNAc concentrations (not shown).

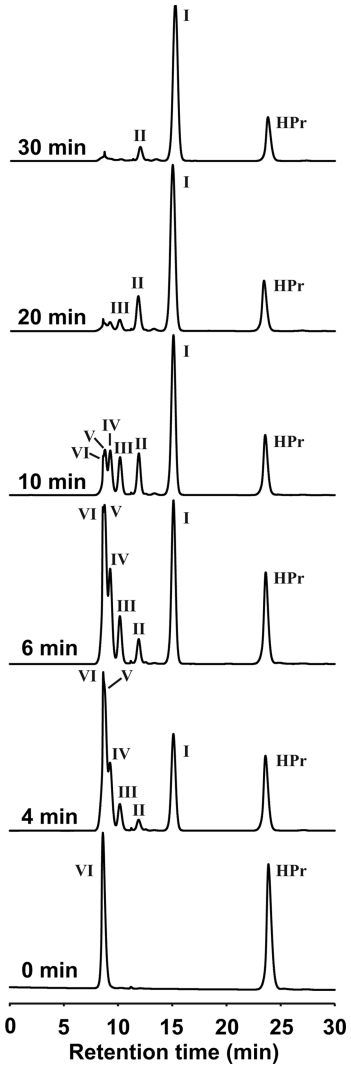

Figure 5. Time-course hydrolysis of $(GlcNAc)_6$ by *Sc*HEX. Samples were analyzed by measuring absorption at 210 nm following an isocratic HPLC separation of products on an Aminex HPX-87H ion exclusion column at 45 °C, as described in Experimental Procedures. Chromatograms are shown for acid-quenched reactions after 0, 4, 6, 10, 20, and 30 min of incubation. Retention times were compared to known chitinooligosaccharide standards: VI, $(GlcNAc)_6$; V, $(GlcNAc)_5$; IV, $(GlcNAc)_4$; III, $(GlcNAc)_3$; II, $(GlcNAc)_2$; I, (GlcNAc); HPr, propionic acid normalization standard.

The *Sc*HEX activity was also tested against longer chain chitins and bulkier substrates, including glycol chitin 80%, glycol chitin 40%, chitosan 24%, chitin crabshell, colloidal chitin, and peptidoglycans from *Bacillus subtilis* and *Streptomyces sp.* After 18 and 24 h of incubation, no significant oligomer was detected in the reaction mixture, except for very low concentrations of GlcNAc (not shown). GlcNAc was not detected in identical assays conducted with the mock supernatant or water as negative controls, confirming that the activity is specific to *Sc*HEX. The bulk of these observations indicate that *Sc*HEX possesses *N*-acetylhexosaminidase activity toward short chain chitin oligomers but not toward long chain chitin or chitosan. This result was expected given the high sequence identity and similar activity observed with other GH20 family members, namely the highly homologous *Sp*HEX.[44] Similar to most other GH20 members characterized, increasing the length and complexity of chitin substrates considerably affects enzyme affinity and catalysis in *Sc*HEX.

Michaelis–Menten Kinetics. *Sc*HEX showed lower specific activity in its purified form than that calculated from the fresh outer-cell growth supernatant immediately after protein expression, most likely due to poor enzyme stability in solution over time. As a result, kinetic parameters were calculated from the 95% pure *Sc*HEX, providing a better portrait of the *in vivo* activity of *Sc*HEX. Considering the high purity of the enzyme in the outer-cell medium and the absence of background activity from the expression organism (as tested from a control *S. lividans* growth assay), this expression system provides a considerable advantage for the industrial production of *Sc*HEX. Indeed, protein purification often cannot be performed in industrial settings due to high costs, setup and productivity issues. The kinetic parameters K_M and k_{cat} were calculated for each chitooligomer under known optimal conditions (see below). Hydrolysis of the substrates showed typical Michaelis–Menten hyperbolic kinetics with substrate concentrations ranging from 0.25 mM to 3 mM (Figure S2). Results show that K_M and k_{cat} parameters are very similar for all substrates, varying from a mere 2- to 3-fold difference in all cases (Table 3). The enzyme displays the lowest affinity toward $(GlcNAc)_2$ (K_M = 1.97 ± 0.42), which correlates with a slightly higher k_{cat} (k_{cat} = 593 ± 94). However, these differences do not translate into higher catalytic efficiency of *Sc*HEX for this substrate and no other significant catalytic efficiency differences were observed for substrate chain lengths ranging from 2 to 6 *N*-acetylglucosamine units $[(GlcNAc)_{2-6}]$. These results demonstrate that substrate affinity is very similar for short

Table 3. Kinetic Parameters for *Sc*HEX

substrate	K_M (mM)	k_{cat} (s^{-1})	k_{cat}/K_M ($mM^{-1}s^{-1}$)
$(GlcNAc)_2$	1.97 ± 0.42	593 ± 94	297 ± 12
$(GlcNAc)_3$	0.76 ± 0.10	330 ± 16	432 ± 25
$(GlcNAc)_4$	0.90 ± 0.15	232 ± 10	258 ± 20
$(GlcNAc)_5$	0.59 ± 0.09	271 ± 1	459 ± 19
$(GlcNAc)_6$	0.98 ± 0.22	409 ± 63	423 ± 63

dx.doi.org/10.1021/bi401697j | *Biochemistry* 2014, 53, 1789–1800

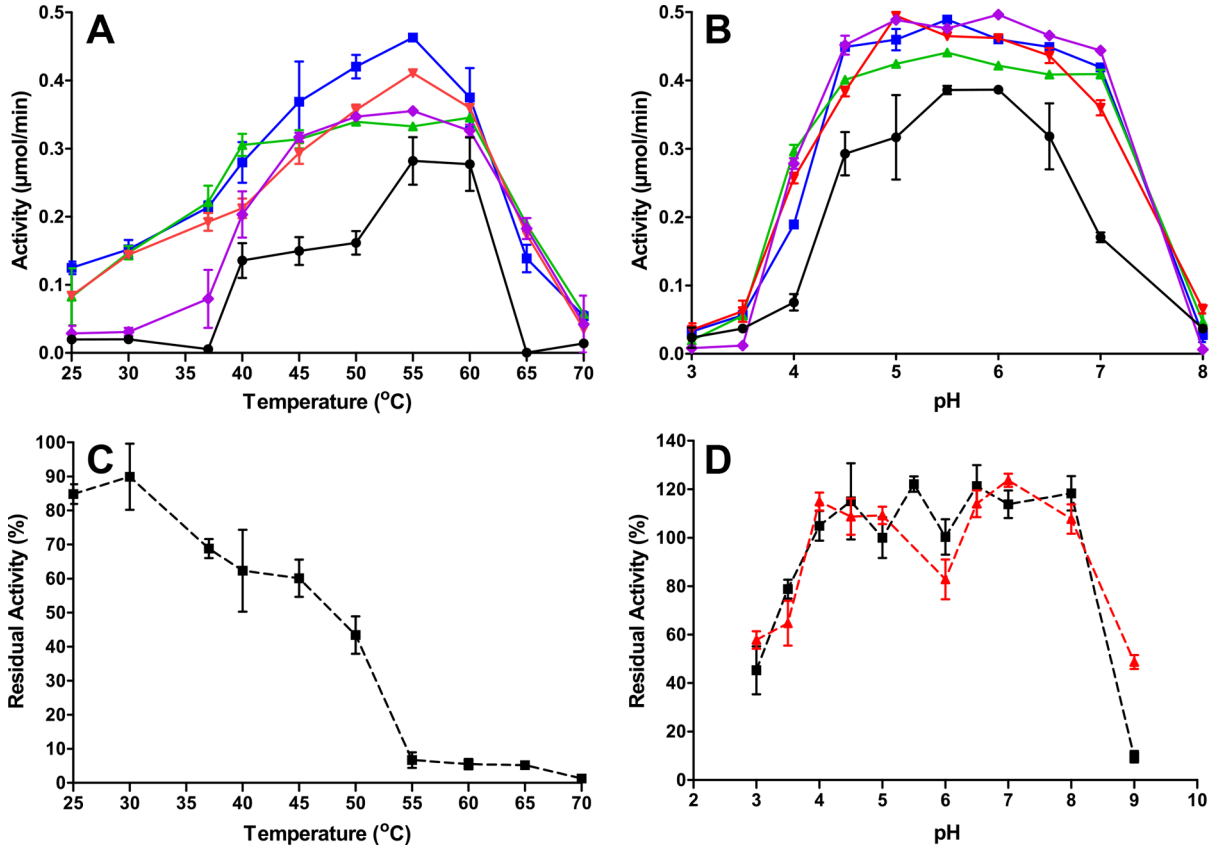

Figure 6. Effect of pH and temperature on *Sc*HEX activity against chitooligosaccharides. (A) Effect of temperature on *Sc*HEX activity. Enzyme activity was tested for $(GlcNAc)_2$ (blue squares), $(GlcNAc)_3$ (green up triangles), $(GlcNAc)_4$ (red down triangles), $(GlcNAc)_5$ (purple diamonds), and $(GlcNAc)_6$ (black circles). (B) Effect of pH on *Sc*HEX activity (same symbols and color code). (C) Residual activity of *Sc*HEX against *p*NP-GlcNAc after a 15-min incubation at various temperatures. (D) Residual activity of *Sc*HEX against *p*NP-GlcNAc after 1 h (black squares) and 3-month (red up triangles) incubation at various pHs. See Experimental Procedures for details.

chitooligomers of varying degrees of polymerization, supporting the observation that *Sc*HEX is an exo-acting glycosidase that cleaves from the nonreducing end of substrates through a processive hydrolytic mechanism, as previously demonstrated on homologues.[3,5,43]

Most GH20 members have been kinetically characterized in the presence of unnatural substrate analogues, such as pNP-GlcNAc, pNP-GalNAc, and/or 4-methylumbelliferyl-β-D-galactopyranosides (4-MUG). Only a restricted set of HEX enzymes has been studied in the presence of natural chitooligomers, including ExoI from *Vibrio furnissii*,[49] *Le*-Hex20A from *Lentinula edodes*,[53] *Vh*Nag from *Vibrio harveyi* 650,[43] and *Stm*Hex from *Stenotrophomonas maltophilia*.[54] The catalytic efficiency of *Sc*HEX compares advantageously with other HEX members, showing very similar k_{cat}/K_M against $(GlcNAc)_{2-6}$ substrates. In fact, *Sc*HEX from crude supernatant is 1700-fold more efficient than pure *Stm*Hex against $(GlcNAc)_6$.[54] Still, even with equal catalytic efficiency, *Sc*HEX remains advantageous from an industrial standpoint due to its chitin degrading ability in the growth supernatant, thus preventing the need for further protein purification.

Enzyme Stability. To provide details on the potential applicability and robustness of *Sc*HEX for the industrial production of GlcNAc, the effect of temperature on activity was determined by monitoring hydrolysis of $(GlcNAc)_{2-6}$ chitooligosaccharides from 25 to 70 °C (Figure 6A). Although *Streptomycetes* are soil-dwelling bacteria that thrive at mesophilic temperatures, *Sc*HEX showed optimal activity at temperatures ranging from 45 to 60 °C with a maximal activity observed at 55 °C for almost all substrates tested. These values are similar to those observed in GH20 members from *Sotalia fluviatilis*,[45] *Streptomyces thermoviolaceus*,[46] *Penicillium oxalicum*,[7] and *Aspergillus oryzae*.[47] Enzyme activity toward $(GlcNAc)_6$ was particularly affected outside the 55−60 °C range (Figure 6A), dropping to near zero at physiological temperatures or lower. The smaller substrates $(GlcNAc)_{2-4}$ were not as affected by drastic temperature drops as $(GlcNAc)_{5-6}$, further lending support to the biological importance of *Sc*HEX in hydrolysis of small chitooligosaccharides in the chitinolytic system of *S. coelicolor* A(3)2.

Thermal stability of *Sc*HEX was also assessed by characterizing enzyme stability after a 15 min incubation at temperatures ranging from 25 to 70 °C prior to reaction initiation (Figure 6C). Despite an optimal activity of 55−60 °C, *Sc*HEX stability at higher temperatures was considerably reduced, dropping dramatically for temperatures higher than that of the optimal growth of its host organism (30 °C). Indeed, while *Sc*HEX retained 43% activity at 50 °C, this efficiency dropped to less than 5−6% when incubated at higher temperatures. This property is similar to NagA from *Pseudomonas fluorescens* JK-0412[5] and β-HEX from *Capsicum annuum*.[48] These results demonstrate the *in vivo* trade-off between enzyme stability and catalytic efficiency, whereby increased stability at lower temperatures is favored over increased enzyme activity. While far from a catalytically perfect enzyme, *Sc*HEX is just good enough to perform its required chitinolytic activity *in vivo*,

dx.doi.org/10.1021/bi401697j | *Biochemistry* 2014, 53, 1789−1800

providing *S. coelicolor* A(3)2 with sufficient enzymatic activity to survive.

The effect of pH on *Sc*HEX activity was also determined by monitoring the hydrolysis of $(GlcNAc)_{2-6}$ chitooligosaccharides from pH 3 to 8 (Figure 6B). *Sc*HEX showed a broad pH tolerance, with optimal activity detected between pH 4.5 and 7. Again, $(GlcNAc)_6$ proved a more stringent substrate by displaying optimal activity between pH 5 and 6.5. Many other GH20 enzymes, such as HEX from *Sotalia fluviatilis*, NagC from *Streptomyces thermoviolaceus*, HEX1 and HEX2 from *Paenibacillus sp.* TS12, and DspB from *Aggregatibacter actinomycetemcomitans*, showed similar optimal activity between pH 5 and 6.[4,39,45,46] Interestingly, ScHEX did not display significant pH-dependent activity variations between chitooligomers of varying degrees of polymerization. This result contrasts with previous observations on β-GlcNAcase and chitodextrinase from *Vibrio furnissii*, two enzymes that showed a shift in pH-activity profiles with the smaller $(GlcNAc)_2$ substrate relative to longer chitin oligomers.[49]

*Sc*HEX also displayed very good residual activity after incubating the enzyme at different pH values for extended periods of time (1 h and 3 months) (Figure 6D). The enzyme maintained almost the same level of activity between pH 4−8 after 1 h or 3 months of incubation in different pH buffer conditions. Additionally, although enzyme activity was significantly affected after 3 months of incubation at 4 °C, *Sc*HEX retained the same residual pH-activity profile as that of the fresh enzyme.

Effect of Carbohydrates on *Sc*HEX Activity. To elucidate the effect of possible activators/inhibitors on catalytic efficiency, *Sc*HEX was preincubated for 15 min in the presence of 3 mM of the following sugars prior to reaction initiation: mannose, fructose, arabinose, glucuronic acid, sucrose, galactose, glucose, xylose, lactose, and GlcNAc. Interestingly, mannose, fructose, glucuronic acid, lactose, and GlcNAc significantly increased enzyme activity by a factor of 33%, 47%, 63%, 28%, and 35%, respectively (Table 4). In contrast, β-*N*-acetylhexosaminidase activity was either unaffected or weakly inhibited by arabinose, sucrose, galactose, glucose, and xylose. The stimulating effect on HEX activity by sugars was also observed in HEX from *Sotalia fluviatilis*, which displayed comparable increases upon incubation with glucuronic acid (65%), fructose (58%), and lactose (70%).[45] While sucrose and galactose do not significantly affect *Sc*HEX activity, both sugars were shown to increase chitinohydrolysis of the *Sotalia fluviatilis* enzyme by 43% and 80%, respectively. Interestingly, preincubation of *Sc*HEX with the reaction product GlcNAc increased enzyme activity by more than 35% relative to control, indicating that product inhibition is not an issue with *Sc*HEX, contrasting with results observed with other GH20 members, namely, *Po*HEX and ExoI from *Penicilium oxalicum* and *Vibrio furnissii*, respectively.[7,49] Overall, the activating effects of fructose and glucuronic acid on *Sc*HEX activity are significant and could be used to enhance the efficiency of the enzyme in GlcNAc production. The exact molecular phenomenon underlying such activation was never investigated in the GH20 family but could result from a potential induced fit and/or conformational selection mechanism triggered by the binding of substrate analogues, thus favoring a catalytically competent enzyme-bound state over the unbound, inactive ground state. This type of ligand binding mechanism was previously characterized on a number of other enzyme systems and has recently attracted considerable attention because both mechanisms may act as a flux and be affected by changes in ligand concentrations.[50]

Table 4. Effect of Carbohydrates on *Sc*HEX Activity

compd	relative activity (%)[a]
control	100
mannose	133 ± 5.3
fructose	147 ± 8.2
arabinose	128 ± 32
glucuronic acid	163 ± 10
sucrose	82 ± 12
galactose	83 ± 12
glucose	104 ± 13
xylose	92 ± 12
lactose	128 ± 14
GlcNAc	135 ± 15

[a]Enzyme assays were carried out with 0.25 mM *p*NP-GlcNAc using *Sc*HEX preincubated for 15 min with 3 mM of each compound. Activities were compared with control, which was performed with pure *Sc*HEX. Results were presented as means ± standard error (n = 3).

CONCLUSION

In the present work, we found that the β-*N*-acetylhexosaminidase from *Streptomyces coelicolor* A3(2) can be produced extracellularly in high yield and with good purity from *S. lividans* cultures. The 3D structure of *Sc*HEX is very similar to that of *Sp*HEX, with which it shares 94% sequence identity. Complexes have been obtained with the inhibitor 6-Ac-Cas and by soaking a catalytic acid/base residue variant of the enzyme, E302Q, with chitobiose. This allowed the capture of the NAG−oxazoline intermediate in the −1 subsite, which binds in a similar manner to the stable inhibitor NAG−thiazoline. The enzyme extract exhibits high chitinolytic activity toward chitooligosaccharides, offering potential for the production of GlcNAc as a chemical precursor. The enzyme demonstrates a wide pH-activity range from 4.5 to 7 and exhibits optimal activity at temperatures up to 55 °C. Kinetic measurements for *Sc*HEX with chitin oligomers showing degrees of polymerization 2−6 have shown k_{cat}/K_M values of a similar order of magnitude. These kinetic parameters are superior or comparable to previously described β-*N*-acetylhexosaminidases, offering an improvement for the industrial application of *Sc*HEX. The release of sequentially shorter chitin oligomeric products from $(GlcNAc)_6$ over time lends support to an exoglycosidase activity, with the enzyme cleaving sugars from the nonreducing end of substrates, as with other GH20 family members. Enzyme activity can be significantly stimulated in the presence of sugars, notably fructose, glucuronic acid, and GlcNAc. Thus, some sugars may be used to increase yield and product inhibition is not an issue. Further work will enable the identification of conditions that can maximize the potential yield of GlcNAc by such an extract in an industrial setting. *Sc*HEX adds to the GH20 repertoire, from a structural and mechanistic standpoint and provides an enabling technology for the high-level bioproduction of monosaccharides.

ASSOCIATED CONTENT

Supporting Information

A sequence alignment of *Sc*HEX with members of the GH20 β-*N*-acetylhexosaminidase family and Michaelis−Menten kinetics profiles for the hydrolysis of $(GlcNAc)_{2-6}$ by *Sc*HEX. This

material is available free of charge via the Internet at http://pubs.acs.org.

Accession Codes

Coordinates and structure factors have been deposited in the Protein Data Bank with accession numbers 4C7D, 4C7F, and 4C7G.

AUTHOR INFORMATION

Corresponding Author

*E-mail: nicolas.doucet@iaf.inrs.ca. Fax: (450) 686-5501. Tel.: (450) 687-5010, ext. 4212.

Author Contributions

The manuscript was written through contributions of all authors. All authors have given approval to the final version of the manuscript.

Funding

This work was supported by a Natural Sciences and Engineering Research Council of Canada (NSERC) Discovery grant (RGPIN 402623-2011), an NSERC Engage grant, and a "Fonds de Recherche Québec−Santé" (FRQS) Research Scholar Junior 1 Career Award (to N.D). N.N.T was the recipient of a Ph.D. scholarship from the "Fondation Universitaire Armand-Frappier de l'INRS". W.A.O. is funded by the United Kingdom Biotechnology and Biological Sciences Research Council (Grant BB/K003836/1).

Notes

The authors declare no competing financial interest.

ACKNOWLEDGMENTS

The authors thank Julie Payet (INRS) for technical assistance and François Lépine (INRS) for mass spectrometry. Data collection was performed at the Diamond Light Source beamlines IO3 and IO4 (Oxfordshire, UK) and staff are thanked for provision of data collection facilities.

ABBREVIATIONS

HEX, β-*N*-acetylhexosaminidase; *Sc*HEX, β-*N*-acetylhexosaminidase from *Streptomyces coelicolor* A3(2); GlcNAc, *N*-acetylglucosamine; GalNAc, *N*-acetylgalactosamine; GH, glycoside hydrolase; *p*NP, *para*-nitrophenyl

REFERENCES

(1) Slamova, K., Bojarova, P., Petraskova, L., and Kren, V. (2010) β-*N*-acetylhexosaminidase: what's in a name...? *Biotechnol. Adv. 28*, 682−693.

(2) Gravel, R. A., Clark, J. T. R., Kaback, M. M., Mahuran, D., Sandhoff, K., and Suzuki, K. (1995) in *The metabolic basis of inherited disease* (Scriver, C. R., Beaudet, A. L., Sly, W. S., and Valle, D., Eds.), pp 1807−1839, McGraw-Hill, Inc., New York.

(3) Kerrigan, J. E., Ragunath, C., Kandra, L., Gyemant, G., Liptak, A., Janoosy, L., Kaplan, J. B., and Ramasubbu, N. (2008) Modeling and biochemical analysis of the activity of antibiofilm agent dispersin B. *Acta Biol. Hung. 59*, 439−451.

(4) Manuel, S. G., Ragunath, C., Sait, H. B., Izano, E. A., Kaplan, J. B., and Ramasubbu, N. (2007) Role of active-site residues of dispersin B, a biofilm-releasing β-hexosaminidase from a periodontal pathogen, in substrate hydrolysis. *FEBS J. 274*, 5987−5999.

(5) Park, J. K., Kim, W. J., and Park, Y. I. (2010) Purification and characterization of an exo-type β-*N*-acetylglucosaminidase from *Pseudomonas fluorescens* JK-0412. *J. Appl. Microbiol. 110*, 277−286.

(6) Mark, B. L., Wasney, G. A., Salo, T. J., Khan, A. R., Cao, Z., Robbins, P. W., James, M. N., and Triggs-Raine, B. L. (1998) Structural and funtional characterization of *Streptomyces plicatus* β-*N*-acetylhexosaminidase by comparative molecular modeling and site-directed mutagenesis. *J. Biol. Chem. 273*, 19618−19624.

(7) Ryslava, H., Kalendova, A., Doubnerova, V., Skocdopol, P., Kumar, V., Kukacka, Z., Pompach, P., Vanek, O., Slamova, K., Bojarova, P., Kulik, N., Ettrich, R., Kren, V., and Bezouska, K. (2011) Enzymatic characterization and molecular modeling of an evolutionarily interesting fungal β-*N*-acetylhexosaminidase. *FEBS J. 278*, 2469−2484.

(8) Jiang, Y. L., Yu, W. L., Zhang, J. W., Frolet, C., Guilmi, A. M. D., Zhou, C. Z., Vernet, T., and Chen, Y. (2011) Structural basis for the substrate specificity of a novel β-*N*-acetylhexosaminidase StrH protein from *Streptococcus pneumoniae* R6. *J. Biol. Chem. 286*, 43004−43012.

(9) Liu, T., Zhang, H., Liu, F., Chen, L., Shen, X., and Yang, Q. (2011) Active-pocket size differentiating insectile from bacterial chitinolytic β-*N*-acetyl-D-hexosaminidases. *Biochem. J. 438*, 467−474.

(10) Mark, B. L., Vocadlo, D. J., Knapp, S., Triggs-Raine, B. L., Withers, S. G., and James, M. N. (2001) Crystallographic evidence for substrate-assisted catalysis in a bacterial β-hexosaminidase. *J. Biol. Chem. 276*, 10330−10337.

(11) Williams, S. J., Mark, B. L., Vocadlo, D. J., James, M. N. G., and Withers, S. G. (2002) Aspartate 313 in the *Streptomyces plicatus* hexosaminidase plays a critical role in substrate-assisted catalysis by orienting the 2-acetamido group and stabilizing the transition state. *J. Biol. Chem. 277*, 40055−40065.

(12) Howard, M. B., Ekborg, N. A., Weiner, R. M., and Hutcheson, S. W. (2003) Detection and characterization of chitinases and other chitin-modifying enzymes. *J. Ind. Microbiol. Biotechnol. 30*, 627−635.

(13) Chen, J. K., Shen, C. R., and Liu, C. L. (2010) *N*-Acetylglucosamine: production and applications. *Mar. Drugs 8*, 2493−2516.

(14) Sashiwa, H., Fujishima, S., Yamano, N., Kawasaki, N., Nakayama, A., Muraki, E., Hiraga, K., Oda, K., and Aiba, S. (2002) Production of *N*-acetyl-D-glucosamine from α-chitin by crude enzymes from *Aeromonas hydrophila* H2330. *Carbohydr. Res. 337*, 761−763.

(15) Pichyangkura, R., Kudan, S., Kuttiyawang, K., Sukwattanasinitt, M., and Aiba, S. (2002) Quantitative production of 2-acetoamodo-2-D-glucose from crystalline chitin by bacterial Chitinase. *Carbohydr. Res. 337*, 557−559.

(16) Saito, A., Fujii, T., Yoneyama, T., Redenbach, M., Ohno, T., and Watanabe, T. (1999) High-multiplicity of Chitinase genes in *Streptomyces coelicolor* A3(2). *Biosci. Biotechnol. Biochem. 63*, 710−718.

(17) Saito, A., Ishizaka, M., Francisco, P. B. J., Fujii, T., and Miyashita, K. (2000) Transcriptional co-regulation of five Chitinase genes scattered on the *Streptomyces coelicolor* A3(2) chromosome. *Microbiology 146*, 2937−2946.

(18) Bentley, S. D., Chater, K. F., Cerdeño-Tárraga, A. M., Challis, G. L., Thomson, N. R., James, K. D., Harris, D. E., Quail, M. A., Kieser, H., Harper, D. B. A., Brown, S., Chandra, G., Chen, C. W., Collins, M., Cronin, A., Fraser, A., Goble, A., Hidalgo, J., Hornsby, T., Howarth, S., Huang, C. H., Kieser, T., Larke, L., Murphy, L., Oliver, K., O'Neil, S., Rabbinowitsch, E., Rajandream, M. A., Rutherford, K., Rutter, S., Seeger, K., Saunders, D., Sharp, S., Squares, R., Squares, S., Taylor, K., Warren, T., Wietzorrek, A., Woodward, J., Barrell, B. G., Parkhill, J., and Hopwood, D. A. (2002) Complete genome sequence of the model actinomycete *Streptomyces coelicolor* A3(2). *Nature 417*, 141−147.

(19) Horsch, M., Mayer, C., Sennhauser, U., and Rast, D. M. (1997) β-*N*-acetylhexosaminidase: a target for the design of antifungal drugs. *Pharmacol. Ther. 76*, 187−218.

(20) Seidl, V. (2008) Chitinases of filamentous fungi: a large group of diverse proteins with multiple physiological functions. *Fungal Biol. Rev. 22*, 36−42.

(21) Saito, A., Shinya, T., Miyamoto, K., Yokoyama, T., Kaku, H., Minami, E., Shibuya, N., Tsujibo, H., and Nagata, Y. E. A. (2007) The *dasABC* gene cluster, adjacent to *dasR*, encodes a novel ABC transporter for the uptake of *N,N,*-diacetylchitobiose in *Streptomyces coelicolor* A3(2). *Appl. Environ. Microbiol. 73*, 3000−3008.

(22) Saito, A., Fujii, T., Shinya, T., Shibuya, N., Ando, A., and Miyashita, K. (2008) The *msiK* gene, encoding the ATP-hydrolysing component of *N,N*9-diacetylchitobiose ABC transporters, is essential

for induction of Chitinase production in *Streptomyces coelicolor* A3(2). *Microbiology 154*, 3358−3365.
(23) Saito, A., Miyashita, K., Biukobic, G., and Schrempf, H. (2001) Characteristics of a *Streptomyces coelicolor* A3(2) extracellular protein targeting chitin and chitosan. *Appl. Environ. Microbiol. 67*, 1268−1273.
(24) Hoell, I. A., Dalhus, B., Heggset, E. B., Aspmo, S. I., and Eijsink, V. G. H. (2006) Crystal structure and enzymatic properties of a bacterial family 19 Chitinase reveal differences from plant enzymes. *FEBS J. 273*, 4889−4900.
(25) Heggset, E. B., Hoell, I. A., Kristoffersen, M., Eijsink, V. G. H., and Vårum, K. M. (2009) Degradation of chitosans with Chitinase G from *Streptomyces coelicolor* A3(2): production of chito-oligosaccharides and insight into subsite specificities. *Biomacromolecules 10*, 892−899.
(26) Caufrier, F., Martinou, A., Dupont, C., and Bouriotis, V. (2003) Carbohydrate esterase family 4 enzymes: substrate specificity. *Carbohydr. Res. 338*, 687−692.
(27) Hurtubise, Y., Shareck, F., Kluepfel, D., and Morosoli, R. (1995) A cellulase/xylanase-negative mutant of *Streptomyces lividans* 1326 defective in cellobiose and xylobiose uptake is mutated in a gene encoding a protein homologous to ATP-binding proteins. *Mol. Microbiol. 17*, 367−377.
(28) Hopwood, D. A., Bibb, M. J., Chater, K. F., Kieser, T., Vruton, C. J., Kieser, H. M., Lydiate, D. J., Smith, C. P., and Ward, J. M. (1985) *Genetic manipulation of Streptomyces—A Laboratory Manual*, The John Innes Foundation, Norwich, U.K.
(29) Ho, S. N., Hunt, H. D., Horton, R. M., Pullen, J. K., and Pease, L. R. (1989) Site-directed mutagenesis by overlap extension using the polymerase chain. *Gene 77*, 51−59.
(30) Winn, M. D., Ballard, C. C., Cowtan, K. D., Dodson, E. J., Emsley, P., Evans, P. R., Keegan, R. M., Krissinel, E. B., Leslie, A. G. W., McCoy, A., McNicholas, S. J., Murshudov, G. N., Pannu, N. S., Potterton, E. A., Powell, H. R., Read, R. J., Vagin, A., and Wilson, K. S. (2011) Overview of the CCP4 suite and current developments. *Acta Crystallogr., Sect. D: Biol. Crystallogr. 67*, 235−242.
(31) McCoy, A. J., Grosse-Kunstleve, R. W., Adams, P. D., Winn, M. D., Storoni, L. C., and Read, R. J. (2007) Phaser crystallographic software. *J. Appl. Crystallogr. 40*, 658−674.
(32) Emsley, P., Lohkamp, B., Scott, W. G., and Cowtan, K. (2010) Features and development of Coot. *Acta Crystallogr., Sect. D: Biol. Crystallogr. 66*, 486−501.
(33) Murshudov, G. N., Vagin, A. A., and Dodson, E. J. (1997) Refinement of macromolecular structures by the maximum-likelihood method. *Acta Crystallogr., Sect. D: Biol. Crystallogr. 53*, 240−255.
(34) Gutternigg, M., Kretschmer-Lubich, D., Paschinger, K., Rendic, D., Hader, J., Geier, P., Ranftl, R., Jantsch, V., Lochnit, G., and Wilson, I. B. (2007) Biosynthesis of truncated N-linked oligosaccharides results from non-orthologous hexosaminidase-mediated mechanisms in nematodes, plants, and insects. *J. Biol. Chem. 282*, 27825−27840.
(35) He, Y., Macauley, M. S., Stubbs, K. A., Vocadlo, D. J., and Davies, G. J. (2010) Visualizing the reaction coordinate of an O-GlcNAc hydrolase. *J. Am. Chem. Soc. 132*, 1807−1809.
(36) http://www.cazy.org/Glycoside-Hydrolases.html. (2013) Glycoside Hydrolase family classification.
(37) Henrissat, B., and Bairoch, A. (1993) New families in the classification of glycosyl hydrolases based on amino acid sequence similarities. *Biochem. J. 293*, 781−788.
(38) Henrissat, B., and Bairoch, A. (1996) Updating the sequence-based classification of glycosyl hydrolases. *Biochem. J. 316*, 695−696.
(39) Sumida, T., Ishii, R., Yanagisawa, T., Yokoyama, S., and Ito, M. (2009) Molecular cloning and crystal structural analysis of a novel *β*-*N*-acetylhexosaminidase from *Paenibacillus* sp. TS12 capable of degrading glycosphingolipids. *J. Mol. Biol. 392*, 87−99.
(40) Intra, J., Pavesi, G., and Horner, D. S. (2008) Phylogenetic analyses suggest multiple changes of substrate specificity within the glycosyl hydrolase 20 family. *BMC Evol. Biol. 8*, 214 DOI: doi:10.1186/1471-2148-8-214.
(41) Jiang, Y. L., Yu, W. L., Zhang, J. W., Frolet, C., Guilmi, A. M. D., Zhou, C. Z., Vernet, T., and Chen, Y. (2011) Structural basis for the substrate specificity of a novel *β*-*N*-acetylhexosaminidase StrH protein from *Streptococcus pneumoniae* R6. *J. Biol. Chem. 286*, 43004−43012.
(42) Prag, G., Papanikolau, Y., Tavlas, G., Vorgias, C. E., Petratos, K., and Oppenheim, A. B. (2000) Structures of chitobiase mutants complexed with the substrate di-*N*-acetyl-D-glucosamine: the catalytic role of the conserved acidic pair, aspartate 539 and glutamate 540. *J. Mol. Biol. 300*, 611−617.
(43) Suginta, W., Chuenark, D., Mizuhara, M., and Fukamizo, T. (2010) Novel *β*-*N*-acetylglucosaminidases from *Vibrio harveyi* 650: cloning, expression, enzymatic properties, and subsite identification. *BMC Biochem. 11*, 40 DOI: doi:10.1186/1471-2091-11-40.
(44) Robbins, P., Overbye, K., Albright, C., Benfield, B., and Pero, J. (1992) Cloning and high-level expression of Chitinase-encoding gene of *Streptomyces plicatus*. *Gene 111*, 69−76.
(45) Gomes, J. E., Souza, D. S. L., Nascimento, R. M., Lima, A. L. M., Melo, J. A. T., Rocha, T. L., Miller, R. N. G., Franco, O. L., Grossi-de-Sa, M. F., and Abreu, L. R. D. (2010) Purification and characterization of a liver-derived *β*-*N*-acetylhexosaminidase from marine mammal *Sotalia fluviatilis*. *Protein J. 29*, 188−194.
(46) Kubota, T., Miyamoto, K., Yasuda, M., Inamori, Y., and Tsujibo, H. (2004) Molecular characterization of an intracellular *β*-*N*-acetylglucosaminidase involved in the chitin degradation system of *Streptomyces thermoviolaceus* OPC-520. *Biosci. Biotechnol. Biochem. 68*, 1306−1314.
(47) Plíhal, O., Sklenár, J., Hofbauerová, K., Novák, P., Man, P., Pompach, P., Kavan, D., Ryslavá, H., Weignerová, L., Charvátová-Pisvejcová, A., Kren, V., and Bezouska, K. (2007) Large propeptides of fungal *β*-*N*-acetylhexosaminidases are novel enzyme regulators that must be intracellularly processed to control activity, dimerization, and secretion into the extracellular environment. *Biochemistry 46*, 2719−2734.
(48) Ghosh, S., Meli, V. S., Kumar, A., Thakur, A., Chakraborty, N., Chakraborty, S., and Datta, A. (2011) The *N*-glycan processing enzymes alpha-mannosidase and beta-D-*N*-acetylhexosaminidase are involved in ripening-associated softening in the non-climacteric fruits of capsicum. *J. Exp. Bot. 62*, 571−582.
(49) Keyhani, N. O., and Roseman, S. (1996) The chitin catabolic cascade in the marine bacterium *Vibrio furnissii:* molecular cloning, isolation, and characterization of a periplasmic *β*-*N*-acetylglucosaminidase. *J. Biol. Chem. 271*, 33425−33432.
(50) Hammes, G. G., Chang, Y. C., and Oas, T. G. (2009) Conformational selection or induced fit: a flux description of reaction mechanism. *Proc. Natl. Acad. Sci. U.S.A. 106*, 13737−13741.
(51) Goujon, M., McWilliam, H., Li, W., Valentin, F., Squizzato, S., Paern, J., and Lopez, R. (2010) A new bioinformatics analysis tools framework at EMBL-EBI. *Nucleic Acids Res. 38*, W695−699.
(52) Potterton, L., McNicholas, S., Krissinel, E., Gruber, J., Cowtan, K., Emsley, P., Murshudov, G. N., Cohen, S., Perrakis, A., and Noble, M. (2011) Developments in the CCP4 molecular-graphics project. *Acta Crystallogr., Sect. D: Biol. Crystallogr. 60*, 2288−2294.
(53) Konno, N., Takahashi, H., Nakajima, M., Takeda, T., and Sakamoto, Y. (2012) Characterization of *β*-*N*-acetylhexosaminidase (LeHex20A), a member of glycoside hydrolase family 20, from *Lentinula edodes* (shiitake mushroom). *AMB Express 2*, 29.
(54) Katta, S., Ankati, S., and Podile, A. R. (2013) Chitooligosaccharides are converted to *N*-acetylglucosamine by *N*-acetyl-*β*-hexosaminidase from *Stenotrophomonas maltophilia*. *FEMS Microbiol. Lett. 348*, 19−25.